PHYSICAL REVIEW B **90**, 245206 (2014)

YbN: An intrinsic semiconductor with antiferromagnetic exchange

H. Warring,[1] B. J. Ruck,[1] J. F. McNulty,[1] E.-M. Anton,[1] S. Granville,[2] A. Koo,[3] B. Cowie,[4] and H. J. Trodahl[1]

[1]*The MacDiarmid Institute for Advanced Materials and Nanotechnology, School of Chemical and Physical Sciences, Victoria University of Wellington, P.O. Box 600, Wellington 6140, New Zealand*

[2]*Robinson Research Institute, Victoria University of Wellington, P.O. Box 33436, Lower Hutt 5046, New Zealand*

[3]*Callaghan Innovation, Lower Hutt, P.O. Box 31310, Lower Hutt 5040, New Zealand*

[4]*Australian Synchrotron, 800 Blackburn Road, Clayton, Victoria 3168, Australia*

(Received 20 October 2014; revised manuscript received 11 December 2014; published 29 December 2014)

We present a study of the structural, conducting, magnetic, and optical properties of YbN thin films. Magnetic measurements reveal an antiferromagnetic Curie-Weiss temperature dependence. We find the temperature-dependent resistivity and carrier concentration to be indicative of YbN being semiconducting in nature. Along with this we observe an absorption onset at 1.5 eV, found from optical transmission and reflection measurements. This apparent combination of antiferromagnetism and semiconductivity present in YbN makes it unique among the rare earth nitrides, a series dominated by ferromagnetic semiconductors.

DOI: 10.1103/PhysRevB.90.245206 PACS number(s): 72.20.−i, 75.50.Pp, 78.20.−e, 71.20.Eh

I. INTRODUCTION

The rare earth nitride series first gained significant experimental interest in the middle of the last century, encouraged by technological developments in lanthanide separation [1–5]. Subsequent progress was hampered by difficulties in achieving full stoichiometry and the materials' propensity to oxidize in ambient conditions. The NaCl structure of the series and the magnetic nature of most were both relatively well characterized using these early samples [6], but with mixed electrical transport data.

More recently, the rare earth nitride series has regained interest with advances in thin film growth and characterization [6]. This accompanies and is motivated by modern theoretical studies of the band structure and magnetic interactions [7,8]. These theoretical studies point towards a wide range of interesting magnetic and electronic properties exhibited by the rare earth nitrides, and the rare earth pnictides as a whole [9,10]. Modern experimental studies have corroborated the earlier magnetic and crystallographic measurements, but have highlighted the fact that many of the early studies which found rare earth nitrides to be semimetallic were probably compromised by poor stoichiometry. It is now widely accepted that most of the series are in fact semiconductors [6,11–20].

The effect of the stoichiometry on the electronic properties can readily be assessed. For a nitrogen density of $\sim 3\times10^{22}$ cm^{-3}, and if each nitrogen vacancy contributes 1–3 electrons to the lattice, only $\approx$1% of the nitrogen sites need to be vacant for a carrier concentration of $(0.3\text{–}1)\times10^{21}$ cm^{-3} to be realized. Carrier concentrations of this magnitude are common among the series, although lower values are frequently observed in GdN samples [11,21,22].

The intrinsic ferromagnetism in a semiconducting series lends interest to the rare earth nitrides which is enhanced by their recent spintronics device integration. Both a GdN field-effect transistor and a superconductor-GdN-superconductor spin filter have been realized [17,22].

The rare earth nitride series comprises contrasting $4f$-shell configurations with both intra- and interionic correlations, with a relatively simple, strongly ionic R^{3+}/N^{3-} rocksalt structure. For those reasons they form a rich playing field for theorists developing treatments of strong correlation in solids, and consequently there are a large number of theoretical treatments of the electronic states across the series [6–8,23,24]. With the paucity of experimental guidance concerning especially the semimetallic versus the insulating state, the theoretical situation remains somewhat uncertain. The generic band structure is determined by the symmetry, with the valence band (VB) maximum at Γ and the conduction band (CB) minimum at X, but theoretical treatments predict variously a small band overlap or finite band gaps.

The most thoroughly studied rare earth nitride is GdN, in which the half-filled $4f$ shell of Gd^{3+} has a purely spin magnetic moment of $7\mu_B$ [6]. It is a semiconductor with a 1.3 eV optical gap at X [25] and an indirect gap between the VB maximum and the CB minimum of $\sim$0.3 eV. The nitride of the next lightest rare earth, EuN, is also a semiconductor, although the $J = 0$ ground state of the trivalent ion prevents ferromagnetic alignment in stoichiometric EuN [24,26]. However, nitrogen vacancies (V_N) introduce divalent Eu^{2+}, with a half-filled $4f$ shell that then harbors the $7\mu_B$ moment characteristic of Gd^{3+} [13,26,27]. EuN becomes a diluted ferromagnetic semiconductor at sufficiently high (>5%) V_N concentration [13,27]. The propensity of Eu to form divalent ions, with half-filled $4f$ shells, has another consequence; the growth of EuN thin films can be accomplished only in the presence of activated nitrogen [27]. In contrast the majority of the rare earth nitrides grow in the presence of unactivated N_2 gas at $\sim10^{-4}$ mbar [6].

YbN provides an interesting comparison and contrast to EuN. It has the same propensity for divalent-ion formation, but unlike Eu^{2+}, Yb^{2+} has a fully occupied $4f$ shell, and thus zero total spin and orbital angular momentum, and zero magnetic moment. Both EuN and YbN are expected to have a single empty $4f$ band threading through and hybridizing with the CB minimum, so with similar heavy $4f$ band behavior interfering with the usual light-mass $5d$ CB states [7]. YbN is furthermore the second-heaviest rare earth nitride, and its consequent small lattice constant suggests a possible small band gap, providing an especially stringent test for the semimetallic versus semiconductor question. It is almost unique among the rare earth nitrides for having been subjected

to a thorough single-crystal investigation more than 20 years ago, in a search for heavy fermion behavior [28]. That study concluded that YbN is antiferromagnetic and semimetallic, although with a carrier concentration consistent with that of an ∼1% off-stoichiometry semiconductor. This is of the same order as the uncertainty in their composition measurement. This antiferromagnetism makes YbN unique among the series of rare earth nitrides dominated by ferromagnets. Here we reexamine YbN using modern thin film growth techniques to shed further light on its magnetic state and electronic structure.

II. EXPERIMENTAL DETAILS

The films studied here were prepared at room temperature in a vacuum system with base pressure 10^{-8} mbar. Yb metal was evaporated by an electron beam at a rate of 0.2–0.5 Å/s under a nitrogen partial pressure of $(1–3)\times10^{-4}$ mbar activated using a Kaufman-type ion source. For electrical transport studies thin (∼100 nm) polycrystalline films were grown on sapphire substrates with pre-deposited Au/Cr electrical contacts, while for other studies single-crystal sapphire or silicon substrates were used. All films were capped with GaN to prevent oxidation.

Magnetic measurements were performed in a Quantum Design superconducting quantum interference device (SQUID) magnetometer, and electrical transport measurements were performed between 300 and 4 K in the van der Pauw geometry using a closed-cycle cryostat. Hall effect studies were conducted using a Quantum Design physical property measurement system. X-ray diffraction (XRD) was undertaken with a Bruker D8 Advance system using a cobalt $K\alpha$ x-ray source with a wavelength of 1.789 Å. The operating voltage of the system was 40 kV with a 35 mA current, and includes a 0.23° parallel-plate-diffracted beam collimator and an incident-beam Goebel mirror to block unwanted x-ray radiation transitions.

Normal-incidence reflection and transmission data were obtained between 1 and 5 eV. A blank substrate and a substrate coated with a nominally identical GaN capping layer were measured in the same way in order to model the data from the GaN/YbN/sapphire sample. The multilayered structure of the film leads to interference effects that are seen as oscillations in the data. In order to extract the complex refractive index the data were compared to calculated reflectance and transmittance spectra obtained using the commercially available program TFCALC [29] which models the multiple reflections. The known layer thicknesses and the optical constants of the substrate and capping layers were kept fixed while the complex refractive index of the film was adjusted to model the measured data.

A film prepared with inert nitrogen had an XRD pattern (Fig. 1) with a (111) peak consistent with Yb metal of lattice parameter 5.46 Å [30]. This film had a room temperature resistivity of 85 $\mu\Omega$ cm with a positive temperature coefficient of resistance (TCR). Thus, unlike some other rare-earth nitrides like GdN, YbN cannot be formed simply by evaporation of Yb in the presence of N_2. To achieve growth of YbN we are then guided by its chemical similarity to EuN, employing the use of activated nitrogen from a dc gridless Kaufman source with a beam energy of 80 eV and ion current of 0.1 A [31]. XRD, displayed in Fig. 1, from one such film grown on sapphire

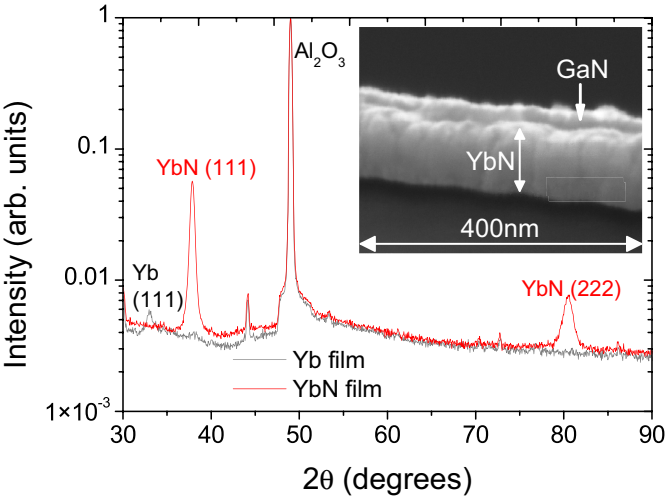

FIG. 1. (Color online) XRD scans for the Yb and YbN films. Inset: SEM image of a YbN film with GaN capping layer on a silicon substrate.

reveals that polycrystalline YbN is formed with a (111) texture and a lattice constant of (4.78 ± 0.01) Å in excellent agreement with previous results [2,6,28]. Scanning electron microscopy (SEM) revealed that the (96 ± 4)-nm-thick film grew in a columnar fashion with column aspect ratio 4 ± 1 (inset to Fig. 1).

The charge state of the Yb ions was probed using x-ray absorption spectroscopy at the Yb M edge (Fig. 2). These data were obtained in the drain current configuration at the soft x-ray beamline of the Australian Synchrotron. The spectrum clearly shows the presence of Yb^{3+} ions, which supports the formation of a nitride and corroborates the XRD data [32]. Yb^{2+} has no M-edge absorption due to a full $4f$ shell, so the signal is entirely due to Yb^{3+} ions.

III. RESULTS

The magnetic response from the YbN film, displayed in Fig. 3, shows an antiferromagnetic Curie-Weiss signal from

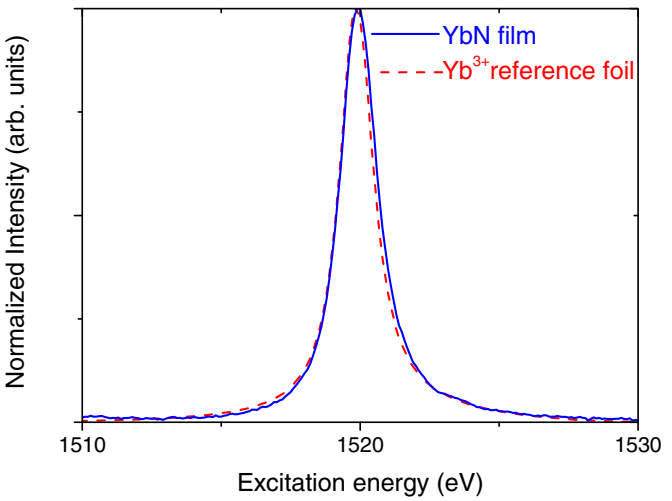

FIG. 2. (Color online) M-edge x-ray absorption spectrum for a YbN film together with a spectrum from a Yb^{3+} reference foil.

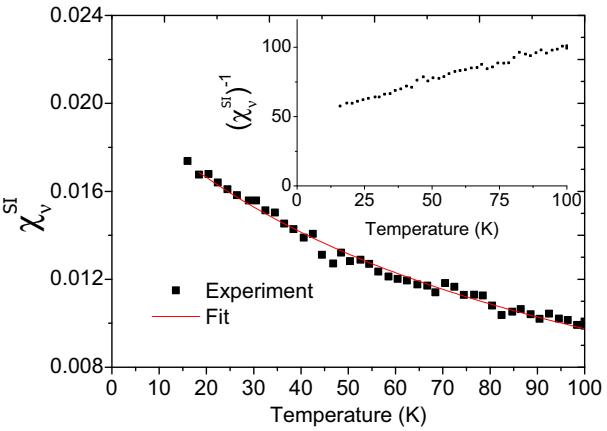

FIG. 3. (Color online) Magnetic susceptibility of YbN measured under an applied field of 250 Oe with the substrate signal subtracted. The data are fitted by a Curie-Weiss law. Inset: Inverse susceptibility with the substrate contribution subtracted.

the YbN. The raw data on the full film structure included contributions from the substrate and capping layer, and we have corrected for those by fitting them to three terms:

$$\chi = \frac{A}{T-\theta} + B + \frac{C}{T}. \quad (1)$$

The first term represents the YbN signal, B represents the known substrate signal, and C signals the presence of a weak Curie-law paramagnetic signal; note that C is an order of magnitude smaller than A. From this we find that the YbN susceptibility is well described by a Curie-Weiss law with $\theta = -93 \pm 3$ K and an effective moment of $(4.5 \pm 0.1)\mu_B$ per Yb^{3+} ion, revealing an antiferromagnetic exchange consistent with previous observations on bulk samples [5,28]. This magnetic moment is in agreement with the expected free-ion value of $g_J\sqrt{J(J+1)} = 4.54\mu_B$ per Yb ion [33], implying that the film is close to stoichiometric with the majority of the Yb ions in the +3 charge state.

Figure 4(a) shows the temperature-dependent resistivity for the YbN sample. The room temperature resistivity of the YbN is about 2.7 mΩ cm and it exhibits a negative TCR. The inset to Fig. 4(a) shows that there is a divergence of the derivative of $\ln\rho$ at low temperatures, which strongly suggests the sample to be insulating in nature. Hall effect measurements, shown in Fig. 4(b), yield an electron concentration of $(1.00 \pm 0.05) \times 10^{21}$ cm^{-3} at room temperature, which gives a mobility of 2.3 cm^2 V^{-1} s^{-1}. This carrier concentration is high and of the same order of magnitude as seen in previous studies of YbN [28]. Note that the Hall effect measurements were carried out in variable fields up to 8 T and there was no evidence of nonlinearity that would indicate transport in multiple bands, as might be expected for a semimetal.

The results of optical reflection (R) and transmission (T) measurements are shown in Fig. 5(a). Strong absorption sets in at energies above about 1.5 eV, although there is still absorption at lower energies as evidenced by values of $R + T$ of about 0.8. The imaginary part of the refractive index is plotted in Fig. 5(b) where the absorption edge at ~1.5 eV is clearly observed along with an upturn at the lowest energies suggestive of free-carrier absorption. Figure 5(b) includes the free-carrier contribution

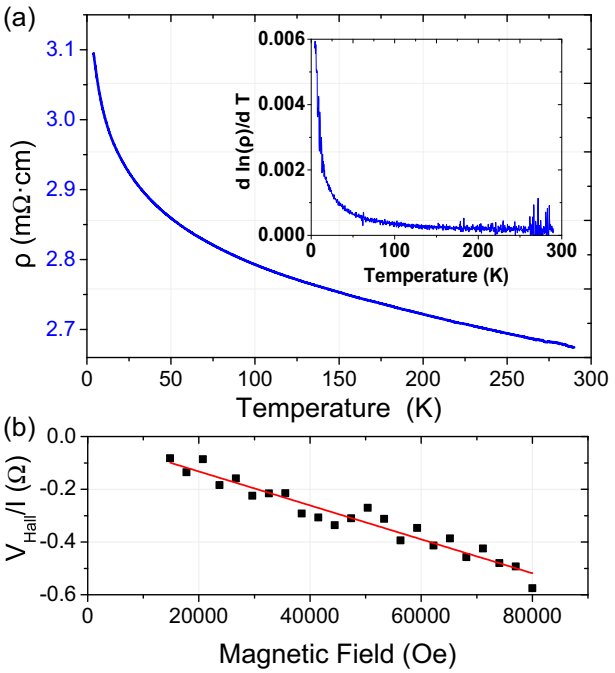

FIG. 4. (Color online) (a) Temperature-dependent resistivity of a YbN film. Inset: Logarithmic derivative of the resistivity plotted against temperature. (b) Hall resistance plotted against magnetic field at 300 K.

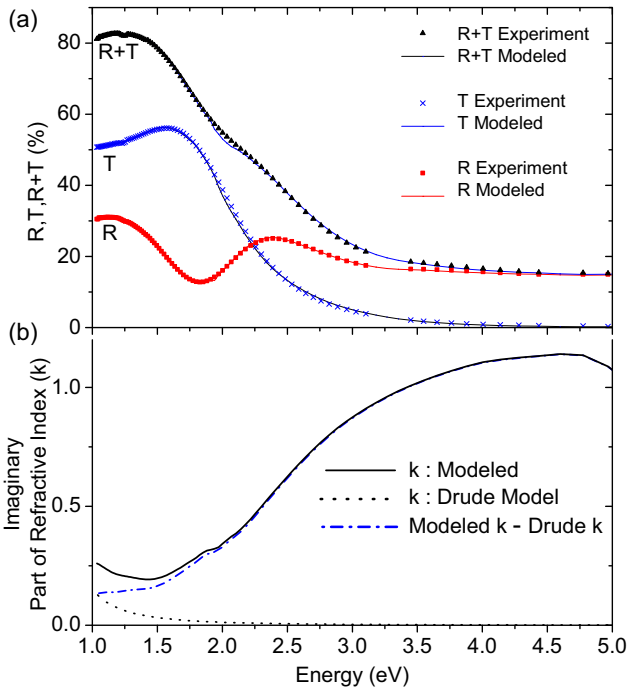

FIG. 5. (Color online) (a) Measured and modeled reflectance (R), transmittance (T), and $R + T$ for a YbN film. (b) Energy dependence of the imaginary part of the YbN refractive index k. The expected Drude contribution to k obtained from the dc transport data is also displayed, along with the overall k with this Drude contribution subtracted.

to k calculated from the Drude model using the parameters obtained from the dc transport data. The estimated free-carrier absorption accounts for the low-frequency upturn.

IV. DISCUSSION

The structural and magnetic properties reported in the present study are consistent with those previously reported. There is, however, a discrepancy in the observed transport properties. This is not uncommon among the rare earth nitrides; even a slightly nonstoichiometric film will cause the sample to be n-type doped while leaving the magnetic and crystallographic properties largely untouched. The low carrier concentration coupled with the room temperature resistivity being well above the Mooij limit is consistent with a doped semiconductor [34]. The TCR in the YbN sample is negative, significantly with a large upturn in the logarithmic derivative at low temperatures that is inconsistent with weak localization in a strongly degenerate electron gas. Thus both of these observations are consistent with an insulating band structure.

The optical data also lend evidence towards YbN being semiconducting in nature. There is a clear onset of absorption at 1.5 eV. However, $R + T$ never exceeds 85% at low energies, or equivalently k is nonzero unless the modeled Drude absorption is subtracted. It is interesting to note that the present values of k (as a function of E) are of similar magnitude to previous results taken from single crystals, although with the onset shifted to higher energies and broadened compared to the previous study [28]. This could be explained by a Moss-Burstein shift due to the enhanced carrier concentration in the present sample, which is also consistent with the larger low-energy absorption.

V. CONCLUSIONS

An investigation into the preparation and properties of YbN thin films has been conducted. We have found that an activated nitrogen precursor is necessary in order for nitridation to occur in YbN films grown at room temperature. This is corroborated by evidence revealing that trivalent Yb is present, along with a lattice constant in agreement with previous studies.

We find that antiferromagnetic exchange is present with $\theta = -93 \pm 3$ K and $\mu_{\text{eff}} = (4.5 \pm 0.1)\mu_B$ per Yb ion, in agreement with previous experiments and with the free-ion Yb^{3+} value. This antiferromagnetic exchange makes YbN unique among the rare earth nitride series for which all other members studied are either para- or ferromagnetic.

The magnitude and negative temperature coefficient of resistance, along with a carrier concentration on the order of 10^{21} cm^{-3} is consistent with a semiconductor doped with a few percent of nitrogen vacancies. This is supported by low-energy absorption present in the optical reflection and transmission data from which we report an optical gap of 1.5 eV.

ACKNOWLEDGMENTS

We acknowledge funding from the New Zealand Foundation for Research, Science and Technology, the Marsden Fund, and the MacDiarmid Institute for Advanced Materials and Nanotechnology, funded by the New Zealand Centres of Excellence Fund. We thank Franck Natali for assistance in film preparation. E.-M.A. thanks the Alexander von Humboldt-Foundation for support through a fellowship.

[1] F. Spedding and A. H. Daane, *The Rare Earths* (John Wiley & Sons, New York, 1961).
[2] W. Klemm and G. Winkelmann, Z. Anorg. Allg. Chem. **288**, 87 (1956).
[3] R. A. Young and W. T. Ziegler, J. Am. Chem. Soc. **74**, 5251 (1952).
[4] F. Endter, Z Anorg. Chem **257**, 127 (1948).
[5] R. Didchenko and F. Gortsema, J. Phys. Chem. Solids **24**, 863 (1963).
[6] F. Natali, B. J. Ruck, N. O. V. Plank, H. J. Trodahl, S. Granville, C. Meyer, and W. R. L. Lambrecht, Prog. Mater Sci. **58**, 1316 (2013).
[7] P. Larson, W. R. L. Lambrecht, A. Chantis, and M. van Schilfgaarde, Phys. Rev. B **75**, 045114 (2007).
[8] C. M. Aerts, P. Strange, M. Horne, W. M. Temmerman, Z. Szotek, and A. Svane, Phys. Rev. B **69**, 045115 (2004).
[9] A. G. Petukhov, W. R. L. Lambrecht, and B. Segall, Phys. Rev. B **53**, 4324 (1996).
[10] C.-G. Duan, R. F. Sabirianov, W. N. Mei, P. A. Dowben, S. S. Jaswal, and E. Y. Tsymbal, J. Phys.: Condens. Matter **19**, 315220 (2007).
[11] S. Granville, B. J. Ruck, F. Budde, A. Koo, D. J. Pringle, F. Kuchler, A. R. H. Preston, D. H. Housden, N. Lund, A. Bittar, G. V. M. Williams, and H. J. Trodahl, Phys. Rev. B **73**, 235335 (2006).
[12] M. Azeem, B. J. Ruck, B. Do Le, H. Warring, H. J. Trodahl, N. M. Strickland, A. Koo, V. Goian, and S. Kamba, J. Appl. Phys. **113**, 203509 (2013).
[13] D. Le Binh, B. J. Ruck, F. Natali, H. Warring, H. J. Trodahl, E.-M. Anton, C. Meyer, L. Ranno, F. Wilhelm, and A. Rogalev, Phys. Rev. Lett. **111**, 167206 (2013).
[14] C. Meyer, B. J. Ruck, A. R. H. Preston, S. Granville, G. V. M. Williams, and H. J. Trodahl, J. Magn. Magn. Mater. **322**, 1973 (2010).
[15] F. Natali, B. Ludbrook, J. Galipaud, N. Plank, S. Granville, A. R. H. Preston, B. L. Do, J. Richter, I. Farrell, R. Reeves, S. Durbin, H. J. Trodahl, and B. J. Ruck, Phys. Status Solidi C **9**, 605 (2012).
[16] D. L. Cortie, J. D. Brown, S. Brück, T. Saerbeck, J. P. Evans, H. Fritzsche, X. L. Wang, J. E. Downes, and F. Klose, Phys. Rev. B **89**, 064424 (2014).
[17] K. Senapati, M. G. Blamire, and Z. H. Barber, Nat. Mater. **10**, 849 (2011).
[18] P. K. Muduli, A. Pal, and M. G. Blamire, Phys. Rev. B **89**, 094414 (2014).
[19] H. Yoshitomi, S. Kitayama, T. Kita, O. Wada, M. Fujisawa, H. Ohta, and T. Sakurai, Phys. Rev. B **83**, 155202 (2011).
[20] I. L. Farrell, R. J. Reeves, A. R. H. Preston, B. M. Ludbrook, J. E. Downes, B. J. Ruck, and S. M. Durbin, Appl. Phys. Lett. **96**, 071914 (2010).

[21] B. M. Ludbrook, I. L. Farrell, M. Kuebel, B. J. Ruck, A. R. H. Preston, H. J. Trodahl, L. Ranno, R. J. Reeves, and S. M. Durbin, J. Appl. Phys. **106**, 063910 (2009).
[22] H. Warring, B. J. Ruck, H. J. Trodahl, and F. Natali, Appl. Phys. Lett. **102**, 132409 (2013).
[23] A. Hasegawa and A. Yanase, J. Phys. Soc. Jpn. **42**, 492 (1977).
[24] M. D. Johannes and W. E. Pickett, Phys. Rev. B **72**, 195116 (2005).
[25] H. J. Trodahl, A. R. H. Preston, J. Zhong, B. J. Ruck, N. M. Strickland, C. Mitra, and W. R. L. Lambrecht, Phys. Rev. B **76**, 085211 (2007).
[26] B. J. Ruck, H. J. Trodahl, J. H. Richter, J. C. Cezar, F. Wilhelm, A. Rogalev, V. N. Antonov, B. D. Le, and C. Meyer, Phys. Rev. B **83**, 174404 (2011).
[27] J. H. Richter, B. J. Ruck, M. Simpson, F. Natali, N. O. V. Plank, M. Azeem, H. J. Trodahl, A. R. H. Preston, B. Chen, J. McNulty, K. E. Smith, A. Tadich, B. Cowie, A. Svane, M. van Schilfgaarde, and W. R. L. Lambrecht, Phys. Rev. B **84**, 235120 (2011).
[28] L. Degiorgi, W. Bacsa, and P. Wachter, Phys. Rev. B **42**, 530 (1990).
[29] Computer code TFCALC 3.5, Software Spectra Inc., Portland, OR, 1993.
[30] B. Beaudry and P. Palmer, J. Less Common Met. **34**, 225 (1974).
[31] I. Kaufman and Robson, *EH200 Ion Source Manual* (Kaufman & Robson, 1306 Blue Spruce Drive Unit A, Fort Collins, CO 80524, 2005).
[32] J. B. Goedkoop, B. T. Thole, G. van der Laan, G. A. Sawatzky, F. M. F. de Groot, and J. C. Fuggle, Phys. Rev. B **37**, 2086 (1988).
[33] J. Van Vleck, *The Theory of Electric and Magnetic Susceptibilities*, International Series of Monographs on Physics (Oxford University Press, Oxford, UK, 1952).
[34] J. H. Mooij, Phys. Status Solidi A **17**, 521 (1973).